



Stiffened Shear Diaphragm Design Requirements for Bracing of Beams

Colter E. Roskos¹, Paul Biju-Duval², Todd A. Helwig³

Abstract

The lateral-torsional buckling capacity of steel girders can be improved with the addition of intermediate bracing. One form of bracing commonly used in the building industry is profiled sheeting that acts as a shear diaphragm to restrain the warping deformation of the top flange. Although metal deck forms are also commonly used in the bridge industry, the forms are not currently permitted to be relied upon for bracing due to flexibility in the connection method. Shear diaphragms attached to the top flange of adjacent girders can be relied on for bracing provided they have adequate stiffness and strength, both of which are sensitive to the connection details. Shear diaphragms may be engaged to act as lateral bracing by connecting the diaphragm along either two or four sides. A common connection detail consists of connecting the diaphragm along two edges that are parallel to the longitudinal axis of the girder and studies have been carried out to develop strength requirements for suitable bracing. Provisions have not been adequately developed in stiffened diaphragms when the stiffening members are perpendicular to the longitudinal axis of the girder. This paper documents a computational study to develop strength requirements for stiffened diaphragms used for stability bracing.

¹ Graduate Research Assistant, University of Texas at Austin, <colter.roskos@utexas.edu>

² Graduate Research Assistant, University of Texas at Austin, <paul.biju-duval@utexas.edu>

³ Professor, University of Texas at Austin, <thelwig@mail.utexas.edu >

1. Introduction

The design of composite steel girders is frequently controlled by the limit state of lateral-torsional buckling which is typically critical during the placement of the concrete deck. During the construction stage, the girders must support the entire construction load until the concrete has adequately cured and can provide lateral and torsional restraint to the top flange of the girders. Therefore, intermediate bracing is often used to reduce the unbraced length of the girders during construction. Unfortunately, the bracing can complicate the girder erection process, and can be relatively expensive to fabricate. In bridge applications, the bracing usually consists of cross frames or diaphragms that can cause fatigue issues in the final bridge where they are no longer needed for stability. The drawbacks of traditional bracing methods in bridges have led researchers to investigate the feasibility of using permanent metal deck forms (PMDF) to continually brace the top flange of girders during construction.

In 2008, a two part paper was published on shear diaphragm bracing of beams with the first part focused on the stiffness and strength behavior and the second part focused on the diaphragm and connection design requirements (Helwig and Yura 2008a, 2008b). In this study, the diaphragms were connected along the two edges that are parallel to the longitudinal axis of the girder and a model was created to estimate how the load flows through the diaphragms and to determine the force in the fasteners that connect the shear diaphragms to the top flanges of the girders. Following the publication of this work, an improved PMDF connection detail was developed for bridge applications that utilized stiffening angles which substantially increase the stiffness of the system (Egilmez 2005).

This paper presents the results of a computational study to gain understanding of the behavior of stiffened PMDF diaphragm systems. The research is applicable to both building and bridge applications in which a shear diaphragm is relied upon for bracing and is connected on all four sides. Specifically, the stiffened diaphragm strength requirements were investigated and a model was created to estimate how the force flows through the stiffened shear diaphragms so that design provisions can be developed for the connections from the PMDF sheets to the stiffening members and for the connections from the stiffening angles to the girders.

2. Background and Previous Work

2.1 Shear Diaphragm Bracing

Lateral-torsional buckling of a girder can be opposed by restraining either the lateral deflection of the compression flange or the twist of the cross-section (Yura 2001). When the compression flanges of two neighboring girders are connected by a shear diaphragm, the girders tend to buckle as a unit and the warping deformations of the flanges are resisted by the presence of the diaphragm. Therefore, the bracing provided by the diaphragm increases the buckling capacity of the girders. One of the first practical solutions for shear diaphragm bracing was produced by two independent studies that were published nearly simultaneously (Errera and Apparao 1976; Nethercot and Trahair 1975). However, the solution was focused on diaphragm braced beams subjected to uniform moment. Helwig and Frank (1999) modified this solution to account for more practical loading conditions resulting in the following equation:

$$M_{cr} = C_b^* M_g + mQd \quad (1)$$

where M_{cr} = buckling capacity of the diaphragm-braced beam; C_b^* = factor for moment gradient that includes effects of load height, if applicable (Helwig et. al 1997; Galambos 1998), M_g = buckling capacity of the girder without the shear diaphragm; m = factor that depends on the loading type; Q = deck shear rigidity, and d = depth of the girder. The deck shear rigidity is expressed as follows:

$$Q = G's_d \quad (2)$$

where G' = diaphragm effective shear stiffness; and s_d = the tributary width of deck bracing a single girder. When a system has n_g girders with a spacing of s_g , the tributary width of the deck bracing a single girder is calculated as:

$$s_d = \frac{n_g - 1}{n_g} s_g \quad (3)$$

The effective shear stiffness and ultimate strength of a diaphragm can be determined experimentally using a cantilever shear frame such as the one depicted in Figure 1. Since the frame is a mechanism on its own, the diaphragm provides all of the lateral stiffness and strength to the system. The effective shear modulus, G' , is derived as follows:

$$G' = \frac{PL}{fw\gamma} \quad (4)$$

where P = lateral load on test frame; L = length of the test frame; f = center to center spacing of loading beams; w = diaphragm width; and γ = diaphragm shear strain.

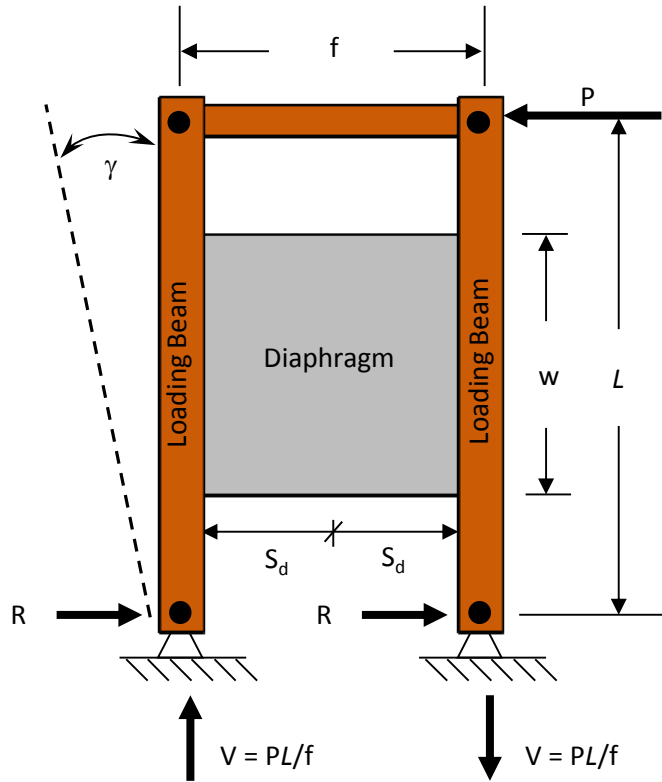


Figure 1: Shear Test Frame with Diaphragm

Suitable bracing must possess adequate stiffness and strength (Winter 1960). Traditionally, the ideal stiffness of a brace is defined as the stiffness required for a perfectly straight member to buckle between the brace points. For stability problems, a larger stiffness than the ideal value is required to control deformation and brace forces. Therefore, Equation 1 must be modified before it can be used for design. For diaphragm braced beams, Helwig and Yura (2008a) recommended that four times the ideal diaphragm stiffness be used for design. Since diaphragm braced beams are essentially continuously braced, the traditional definition of “buckling between the braced points” was not meaningful. Therefore, the ideal stiffness for diaphragm braced beams was based upon the stiffness required to reach a given load or stress level (Helwig and Yura 2008a). While a given stress limit is somewhat arbitrary, a value such as 50 ksi (or the yield stress of the material under consideration) would be a practical limit. For a given maximum factored moment, M_u , the previous expression can be utilized to obtain the following design equation:

$$M_u = C_b^* M_g + \frac{mG' s_d d}{4} \quad (5)$$

In addition to establishing the diaphragm stiffness requirements, Helwig and Yura (2008b) developed the following equation (from parametric study of three different sections at three different span-to-depth ratios) to determine the maximum warping restraining moment per unit length along the longitudinal axis of the girder, $M'_{br,max}$:

$$M'_{br_max} = 0.001 \frac{M_u L}{d^2} \quad (6)$$

where M_u = maximum design moment along the diaphragm braced beam; L = spacing between discrete bracing points that prevent twist; and d = beam depth. Equation 6 above was developed using a large displacement analysis on an imperfect system with the diaphragm stiffness set at four times the ideal value. Notional loads were used to create the imperfection in the top flange while keeping the bottom flange straight which previously studies have shown to represent the critical shape imperfection for beam bracing problems (Wang and Helwig 2005). The maximum twist imperfection at midspan was set to $\vartheta_o = L/(500d)$ which is conservatively twice the value of the $\vartheta_o = L/(1000d)$ which is consistent with imperfection limits from the AISC Code of Standard Practice (AISC 2010).

The moment and shear on an unstiffened PMDF diaphragm are calculated as $M_{br} = M'_{br}L_d$ and $V_{br} = 2M_{br}/w_d$, respectively where L_d is the length of the diaphragm segment and w_d is the width of the diaphragm segment (see Figure 2). These equations are based on the assumptions that the unstiffened PMDF sheets act independently from one another even though they are connected by intermediate sidelap fasteners. In laboratory tests performed by Egilmez et al. (2005), the unstiffened PMDF sheets were observed to act in this manner.

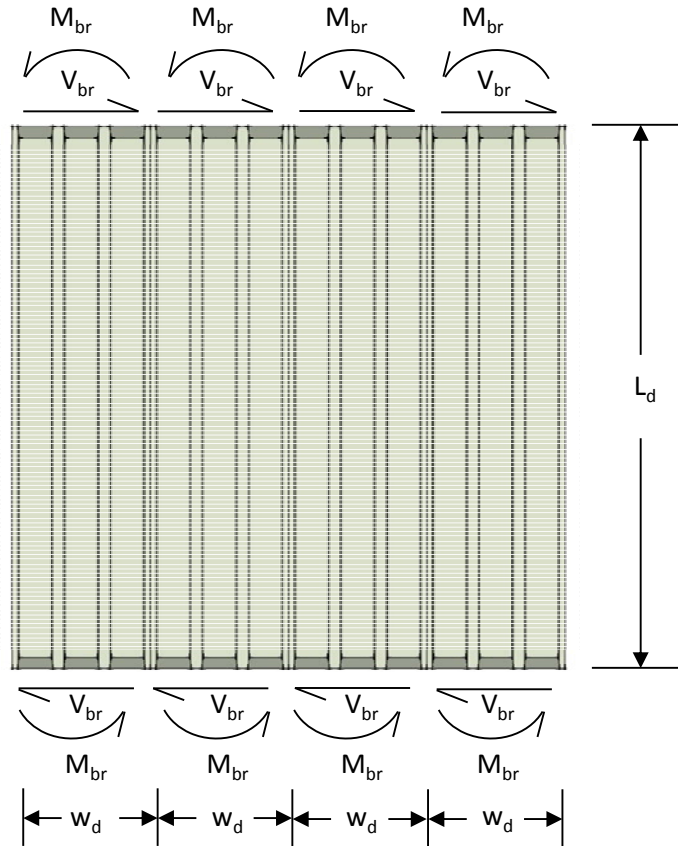


Figure 2: Behavior of Unstiffened Diaphragm

2.1 Stiffened and Unstiffened PMDF Diaphragms

In the building industry, PMDFs are often relied upon to laterally brace beams during construction. The large in-plane shear stiffness of PMDFs can effectively restrain the warping deformation of the beams only if an adequate connection is developed between the PMDFs and the girders. Since the top flange of adjacent beams are typically at the same elevation in buildings, PMDFs span continuously across the top of the beams and are connected directly to the flange via mechanical fasteners, puddle welds, or shear studs as shown in Figure 3a. In the bridge industry, however, the elevation of the top flange often differs between adjacent girders due to differential camber and along the length of a girder due to a change in the flange thickness (aka a haunch). To maintain a constant deck thickness, angles that support the PMDF are welded to the top flange at different heights to accommodate the elevation difference in the flanges as shown in Figure 3b. The support angle eccentricity is defined as the distance from the bottom of the PMDF to the closest face of the top flange. While the support angle connection is quite stiff in the direction parallel to the span of the girder, the angle is flexible and can easily bend when loaded perpendicular to the span of the angle. Currah (1993) showed that the support angle eccentricity substantially decreased the stiffness of the shear diaphragm system.

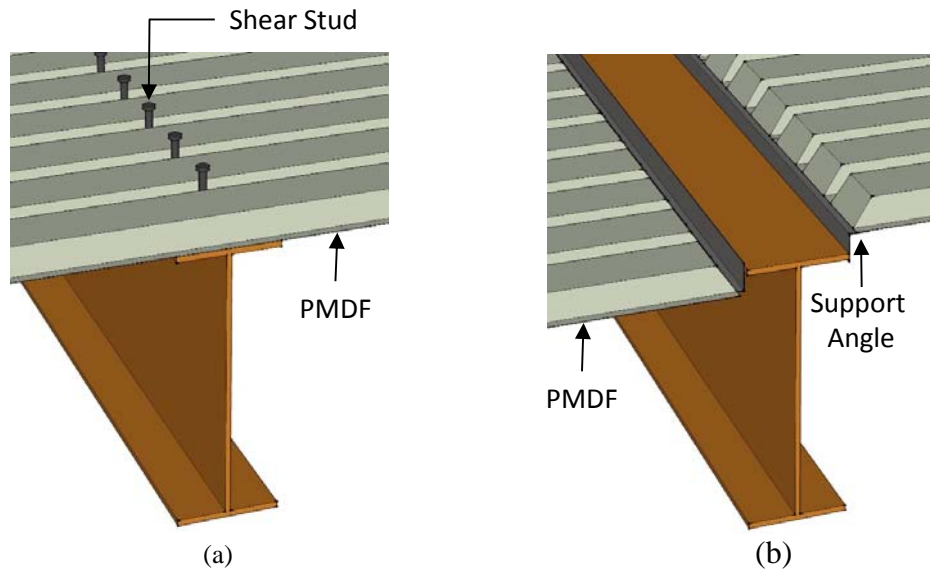


Figure 3: Typical PMDF Connection in (a) Buildings (b) Bridges

To increase the connection stiffness perpendicular to the span of the girder, Egilmez (2005) added stiffening angles to the PMDF diaphragm system as shown in Figure 4. The stiffening angles spanned between the adjacent girders and were connected to a member attached to the top flange. The angles were placed at the lap splice of two neighboring PMDFs so that one screw would penetrate both PMDFs and fasten them to the stiffening angle. While the addition of the stiffening angle significantly increased the stiffness of the PMDF/connection system, it also altered the system's load path. Therefore the following parametric study was performed to determine how the load flows through the stiffened PMDF diaphragm system.

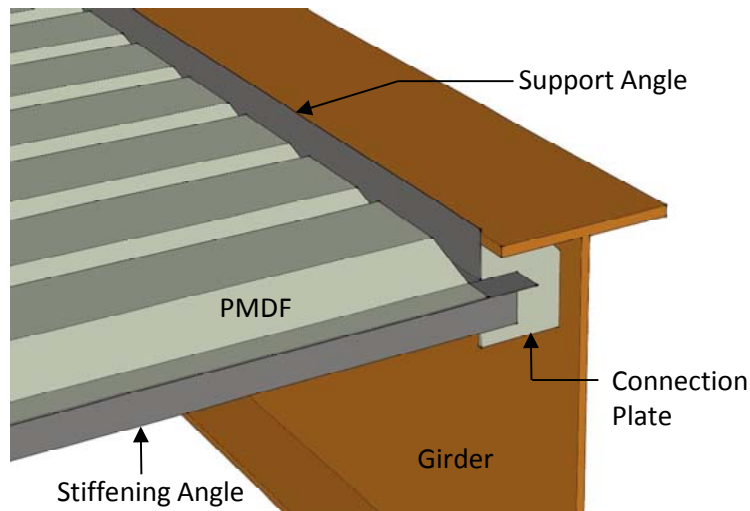


Figure 4: PMDF Connection with Stiffening Angles

3. Finite-Element Model

Abaqus 6.13 was used to conduct parametric studies on a system of simply supported twin girders that were connected by a shear diaphragm at the top flange. In all analyses, linear elastic materials were used for all components of the model. Since the shear diaphragm bracing for forming systems is primarily active during construction, the assumption of elastic behavior is reasonable. For applications involving significant inelasticity, the solutions provide a good starting point for the bracing requirements; however additional investigation is necessary. While the PMDFs in reality are connected to the edge of the girder, the PMDFs were connected to the nodes at the flange/web intersection for simplicity and this model is consistent with the mechanical representation of the shear diaphragm where the bracing restrains warping deformation of the top flange.

3.1 FEA Girder Model

For the girder model, two finite elements were used across the width of the flanges and four elements were used through the depth of the web. Vertical web stiffeners that matched the flange width having four elements through the depth were used at each support to prevent web buckling from the concentrated reaction. The aspect ratio of the elements were maintained to values less than 1:2 for all analyses in this study. The girders and vertical web stiffeners were modeled using an 8-node doubly curved thin shell element with reduced integration and five degrees of freedom per node (aka S8R5 in Abaqus 6.13). At both ends, the girders were supported vertically and horizontally at the web to bottom flange intersection while only one end was fixed longitudinally to create the conventional simply supported pinned-roller condition. Twist of the cross section was prevented by horizontally pinning the top of the beam at the web to top flange intersection, creating a warping permitted connection.

Uniform load distributed along the length of the girder was the only load case considered in the analysis. All of the load was applied at the top flange to web intersection since the majority of the construction load flows into the girders at this location with exception to the girders self-weight. Furthermore, loading a girder at the top flange decreases the buckling capacity of the girder due to second-order effects and is therefore a conservative assumption. Both girders were equally loaded in the analysis even though the system is expected to behave as a lean-on system

(i.e. the buckling capacity of the system is equal to the sum of the buckling capacity of the components regardless of the load distribution between the adjacent girders) as mentioned by Helwig and Yura (2008a).

3.1 FEA Stiffened Diaphragm Model

The stiffened shear diaphragm was modeled using cross-frames built up from linear two-node three-dimensional truss elements that can act in both tension and compression. For reference, Figure 5 shows a plan view of the truss model. The PMDF sheets are modeled using the cross-frames (XF) that are connected to the centerline of the girders top flange. The stiffening angles are simulated using a rigid beam that is pinned to the centerline of the girders top flange and connected to the stiffening cross-frame (SXF).

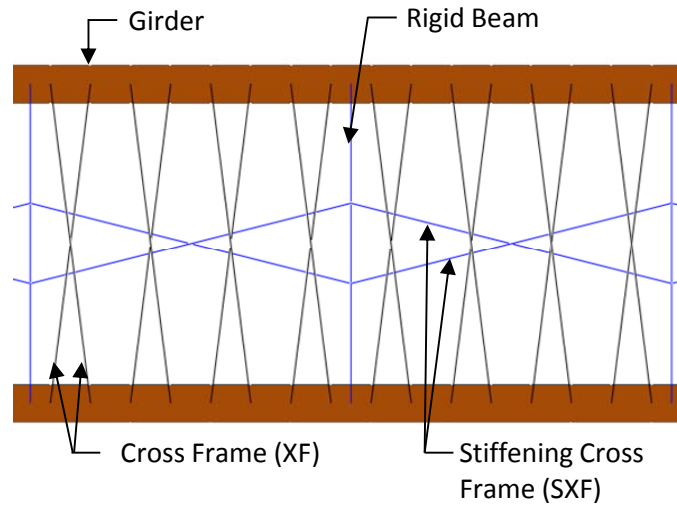


Figure 5: Plan View of Finite Element Stiffened Diaphragm Model

In his work on the fundamentals of beam bracing, Yura (2001) derived an equation to determine the in-plane stiffness of a tension-compression cross-frame system. This equation can be used to determine the stiffness of both the XF and the SXF as follows:

$$\beta_{xf} = \frac{A_{xf} E s_g^2 h_{xf}^2}{L_{xf}^3} \quad (7)$$

$$\beta_{sxf} = \frac{A_{sxf} E s_s^2 h_{sxf}^2}{L_{sxf}^3} \quad (8)$$

where β_{xf} = stiffness of the XF (kip·in/rad); β_{sxf} = stiffness of the SXF (kip·in/rad); A_{xf} = area of the XF elements; A_{sxf} = area of the SXF elements, E = modulus of elasticity; s_g = center to center spacing of the girders; s_s = center to center spacing of the stiffening angles; h_{xf} = horizontal distance between ends of XF members; h_{sxf} = horizontal distance between ends of SXF members; L_{xf} = length of the XF members; and L_{sxf} = length of the SXF members. The relative stiffness of the XF and the SXF is controlled by changing the area of the corresponding truss elements. The shear rigidity of the XF, Q_{xf} , and the shear rigidity of the SXF, Q_{sxf} , can be calculated as follows:

$$Q_{xf} = \frac{\beta_{xf}}{s_{xf}} \quad (9)$$

$$Q_{sxf} = \frac{\beta_{sxf}}{s_s} \quad (10)$$

where s_{xf} = center-to-center spacing between adjacent XF. For the purposes of the research in this paper, $s_{xf} = 2h_{xf}$. The total shear rigidity of the stiffened PMDF diaphragms, Q_{total} , is calculated as the sum of the contributing parts:

$$Q_{total} = Q_{xf} + Q_{sxf} \quad (11)$$

The relative shear rigidity of the XF to the total shear rigidity, q_{xf} , and the relative shear rigidity of the SXF to the total shear rigidity is taken as:

$$q_{xf} = \frac{Q_{xf}}{Q_{total}} \quad (12)$$

$$q_{sxf} = \frac{Q_{sxf}}{Q_{total}} \quad (13)$$

4. Relative Shear Rigidity of Stiffened Diaphragm Components

The relative shear rigidity of the XF and SXF can be determined from experimental results from Egilmez et al. (2009). In these experiments, a full-scale laboratory test was performed on a twin girder system that was braced by several different PMDF diaphragm configurations – with and without stiffening angles. To measure the stiffness of the simply supported twin girder and PMDF diaphragm systems, lateral loads were applied at the quarter points and/or the midpoint of the top flanges and the corresponding lateral deflections were recorded at these points. A singly symmetric cross-section was used for the girders that was created by flame cutting the top flange of a W30x90 down to a 6.25 in. width from its original 10.4 in. width. The twin girder system spanned 49 ft. - 5 in. and the center-to-center spacing of the girders was 9 ft. - 7-¼ in. Three different thickness values of the PMDF sheets were tested in this study (20ga, 18ga, 16ga) and the PMDF sheets were 3 in. deep with an 8 in. pitch. Cold formed L3x2x10ga and L3x3x10ga were used as support angles for the PMDF sheets and as stiffening angles. These support angles were welded to the top flange of the girder at the maximum expected eccentricity of 2.75 inches. Stiffened PMDF diaphragms with support angles at 8, 16, and 24 ft were tested along with unstiffened PMDF diaphragms.

To determine a realistic value of the relative shear rigidity of the XF vs the SXF, a FEM of the twin girder system outlined above was created as shown in Figure 6. First, the FEM excluded the stiffening truss panel and the area of the XF was adjusted until the lateral stiffness of the system matched the experimental results for the unstiffened PMDF diaphragm test. Next, the SXF were added to the system and the area of their members was increased until the lateral stiffness of the system matched the experimental results for the stiffened PMDF diaphragm test. Thus, the shear rigidity for both the XF and the SXF could be calculated. The case that was considered used an 18ga thick PMDF with L3x2x10ga support and stiffening angles. Table 1 shows the lateral

stiffness from the laboratory test and the lateral stiffness from the FEM for the unstiffened PMDFs and the PMDFs with stiffening angles at 8 ft. on center. The effective shear modulus and the total shear rigidity was calculated for both cases using the results from the calibrated FEM. For the case described above, q_{xf} and q_{sxf} were approximately 0.45 and 0.55, respectively. The understanding of realistic values for q_{xf} and q_{sxf} will help define the parameters of the following parametric study.

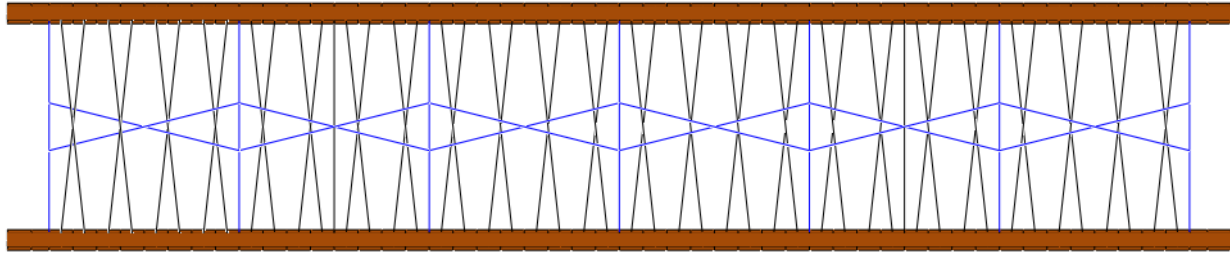


Figure 6: Plan View of FEA Model for Comparison with Experimental Results

Table 1: FEA Results Compared to Experimental Results

Type of PMDF System	Partial Deck		Full Deck		Full Deck		G' Equation	Q _{total} Equation
	Quarter Point Loading		Quarter Point Loading		Midspan Loading			
	LAB (kip/in)	FEM (kip/in)	LAB (kip/in)	FEM (kip/in)	LAB (kip/in)	FEM (kip/in)		
Unstiffened	18.8	18.8	17.4	18.8	11.4	10.1	13.0	703.9
Stiffening Angles @ 8'	34.8	34.8	34.0	34.8	19.3	20.0	28.0	1556.2

(Egilmez et al. 2009)

5. Parametric Study

Two different sections were considered in this study as shown in Figure 7. Section 1 is simply a W16x26 (neglecting the fillets of the beam) while Section 2 is the same a W16x26 with its flange width increased by a factor of 1.5 (from 5.5 in. to 8.25 in.). Section 1 was purposely the same as one of the sections used in the parametric study by Helwig and Yura (2008b) as the research in this paper is intended to build upon the foundation of the previous work. As explained by Helwig and Yura (2008b) the W16x26 was used since it has one of the most slender webs of the standard rolled sections and will therefore produce conservative results for sections with stockier webs.

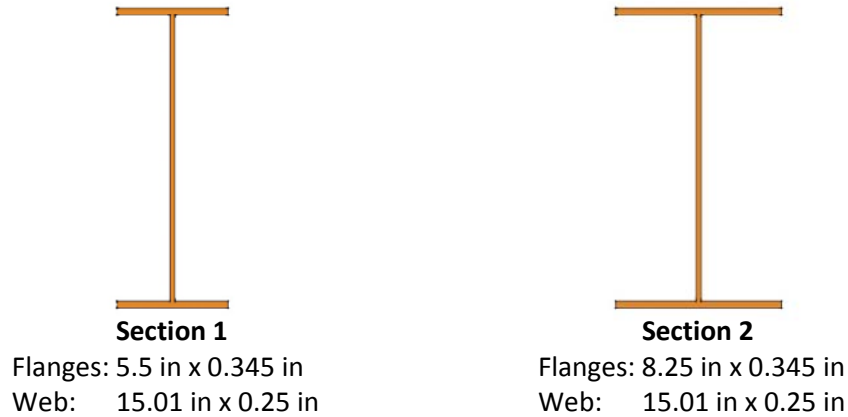


Figure 7: Sections for Parametric Study

Four different span to depth ratios (L/d) for each section were considered in this analysis, namely 15.3, 19.9, 24.5, and 26.0. As the span of the twin girder system increased, more XFs and SXFs were required. As shown in Figure 8, 20, 26, 32, and 34 XFs and 5, 6, 8, and 8 SXFs were used for the span to depth ratios of 15.3, 19.9, 24.5, and 26.0, respectively. Finally, three different stiffness parameters were included in the study where the proportional shear rigidity of the XFs and SXFs were varied as follows: Case 1: $q_{xf} = 1.0$ and $q_{sxf} = 0$, Case 2: $q_{xf} = 0.75$ and $q_{sxf} = 0.25$, and Case 3: $q_{xf} = 0.5$ and $q_{sxf} = 0.5$. Therefore, 24 different models in total (2 sections x 4 L/d ratios x 3 Cases) were used for the parametric study.

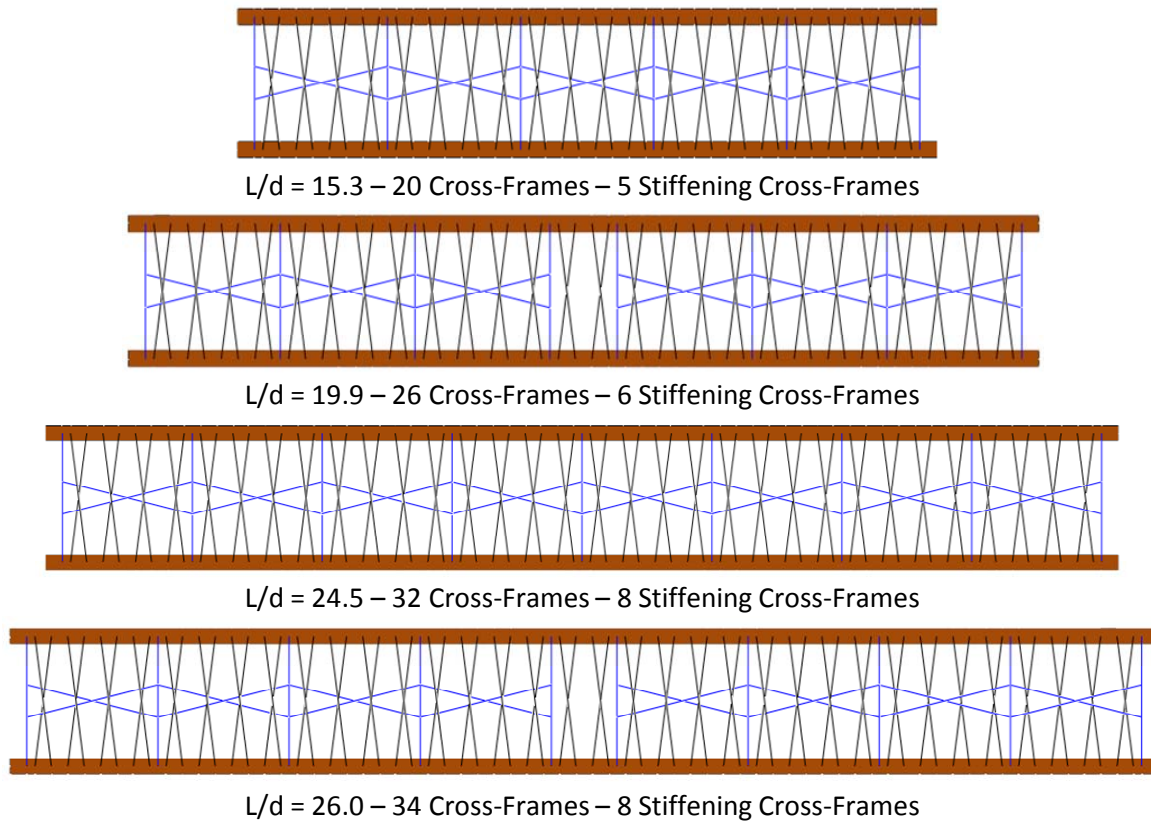


Figure 8: Plan View of Models for Parametric Study

For consistency with the aforementioned work by Helwig and Yura (2008b), the ideal diaphragm stiffness was determined from an eigenvalue buckling analysis of a perfectly straight system that carried uniform loads of equal proportion along the web to top flange intersection of the two girders. The magnitude of the load was such that it produced a maximum bending stress of 50 ksi at midspan of the girders. The diaphragm strength requirements were determined from a large-displacement analysis carried out on an imperfect system using a diaphragm stiffness of four times the ideal value. The twist imperfection at midspan was set to $\theta_o = L/(500d)$ and the imperfect system was created by setting the diaphragm stiffness equal to zero and running an eigenvalue buckling analysis with the bottom flanges of the girders supported horizontally along their length. The buckled shape was then scaled and imported into the model for the large displacement analysis in a manner that did not stress the girders, the XF members, or the SXF members.

6. Maximum Bracing Moments along the Length of the Girder

For Section 1 and Case 1 (where all of this stiffness was present in the XF) the results theoretically should be identical to those given by Helwig and Yura (2008b). Therefore, the maximum value for the warping restraining moment per unit length along the length of the girders of the XF, $M'_{br_xf_max}$, should equal to the value shown in Equation 6 above. Figure 9 shows the normalized $M'_{br_xf_max}$ value for the four different span-to-depth ratios as the load on the beam was increased from zero until the girder moment reached M_{max} . While Equation 6 was validated for L/d of 13.5 and 19.9, $M'_{br_xf_max}$ exceeded the value in the equation for L/d of 24.5 and 26.0. In fact for $L/d = 26.0$, the FEM did not converge for the case of $M/M_{max} = 1.0$. This result was somewhat unexpected since M'_{br_max} in the study by Helwig and Yura (2008b) never exceeded the value in Equation 6 even for $L/d = 25$. The discrepancy could possibly be attributed to the difference in how the imperfections were applied in this study (imported buckled shape) versus the notional load used in the previous study by Helwig. The present study, however, does indicate that at large L/d ratios Equation 6 may become unconservative. As the beams began to buckle at the larger L/d ratios of 24.5 and 26.0, a substantial amount of twist was observed at the midspan of the beam with the lateral deflection of the bottom flange exceeding that of the top flange by more than a factor of two. Thus, it was expected that increasing the width of the flanges (which in turn would increase the beams weak axis stiffness and torsional stiffness) would decrease the lateral deflections of the flanges, reducing the required bracing moment.

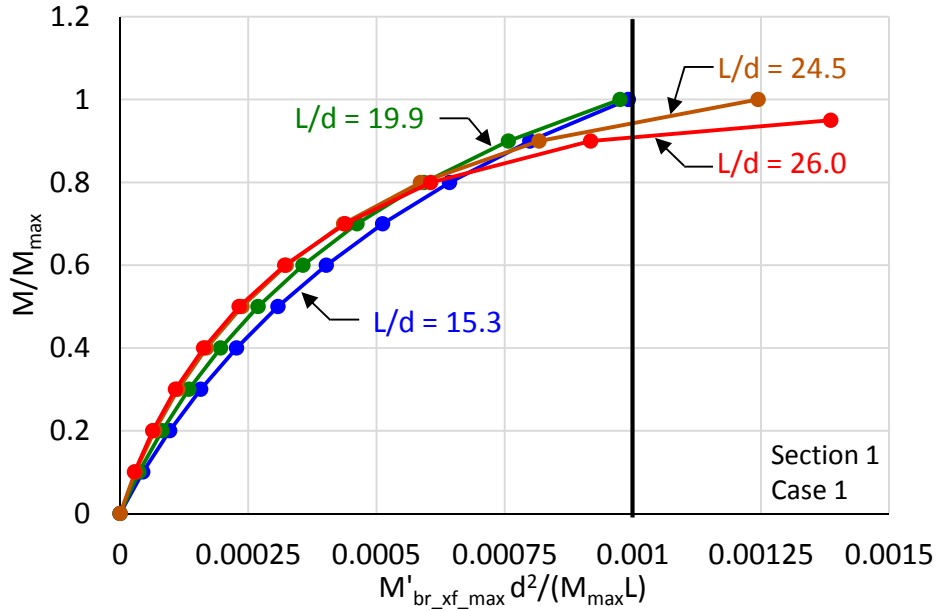


Figure 9: Maximum Normalized Brace Moments for Section 1

The results from the investigation of Case 1 for Section 2 are presented in Figure 10. Recall that Section 2 is the same as Section 1 but with the flanges increased by a factor of 1.5. With the increased flange width, $M'_{br_xf_max}$ along the length of the girders for all L/d ratios was reduced, and convergence was reached at the L/d ratio of 26.0. Therefore, $M'_{br_xf_max}$ along the length of the beam is dependent on more than M_u , L , and d as indicated by Equation 6, however, more research is needed before the exact relationship with the weak axis stiffness and/or torsional stiffness of the girders can be stated.

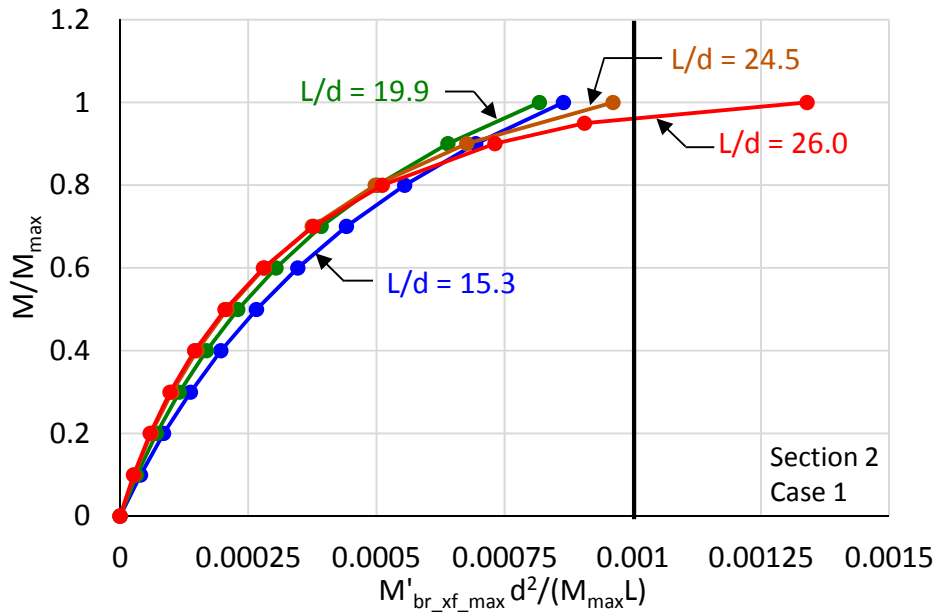


Figure 10: Maximum Normalized XF Brace Moments for Section 2

7. Effect of Relative Shear Rigidity on Brace Moment Distribution

To display how changing the relative shear rigidity of the XF and the SXF affects the forces in the 24 FEA models, the results from the model using Section 1 with $L/d = 19.9$ will be explained in detail. Figure 11 shows the normalized brace moments in the XF, M'_{br_xf} , along the girder for the three different cases where the shear rigidity varies. Since the girders are symmetric about the centerline, the brace moments are only graphed over half of the span where x = the distance from the girder's support. As the proportional shear rigidity, q_{xf} , of the XF decreases from Case 1 to Case 3, M'_{br_xf} also decreases. Further normalizing M'_{br_xf} by q_{xf} causes the three curves for the three different stiffness ratios to virtually coincide as shown in Figure 12. Therefore, M'_{br_xf} is directly proportional to the shear rigidity of the UTP and $M'_{br_xf_max}$ can be calculated as follows:

$$M'_{br_xf_max} = 0.001 \frac{M_u L q_{xf}}{d^2} \quad (14)$$

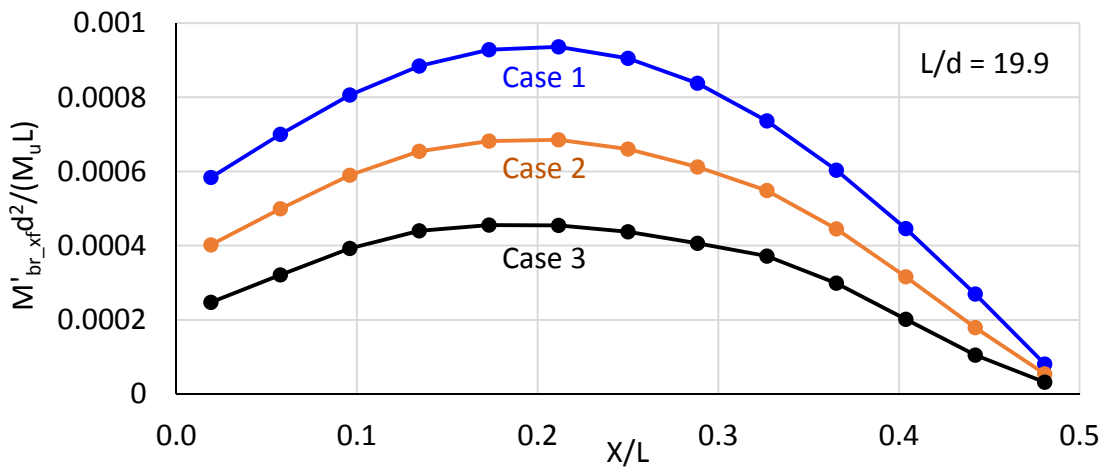


Figure 11: Normalized XF Brace Moments along Girder Length

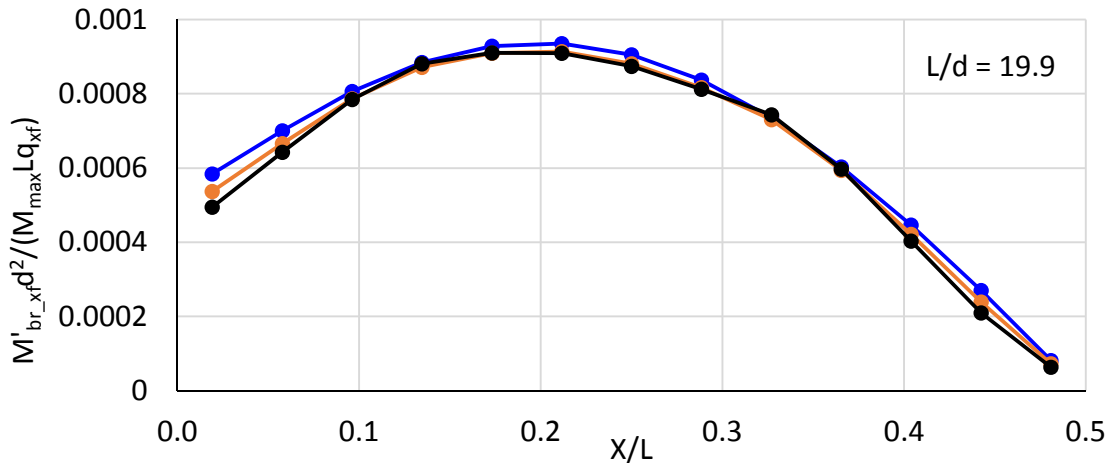


Figure 12: Further Normalized XF Brace Moments along Girder Length

Similar to the XF, the forces in the SXF also vary as the shear rigidity of the SXF changes as shown in Figure 13. As the proportional shear rigidity of the SXF, q_{sxf} , increases from Case 1 to Case 3, M'_{br_sxf} also increases. Further normalizing M'_{br_sxf} by q_{sxf} caused the two curves for the

Case 2 and Case 3 to fall on top of one another as shown in Figure 14 (Case 1 cannot be normalized by q_{sxf} because it would cause zero to appear in the denominator of the fraction). Therefore, M'_{sxf_br} is directly proportional to the shear rigidity of the SXF and $M'_{br_sxf_max}$ can be calculated as follows:

$$M'_{br_sxf_max} = 0.001 \frac{M_u L q_{sxf}}{d^2} \quad (15)$$

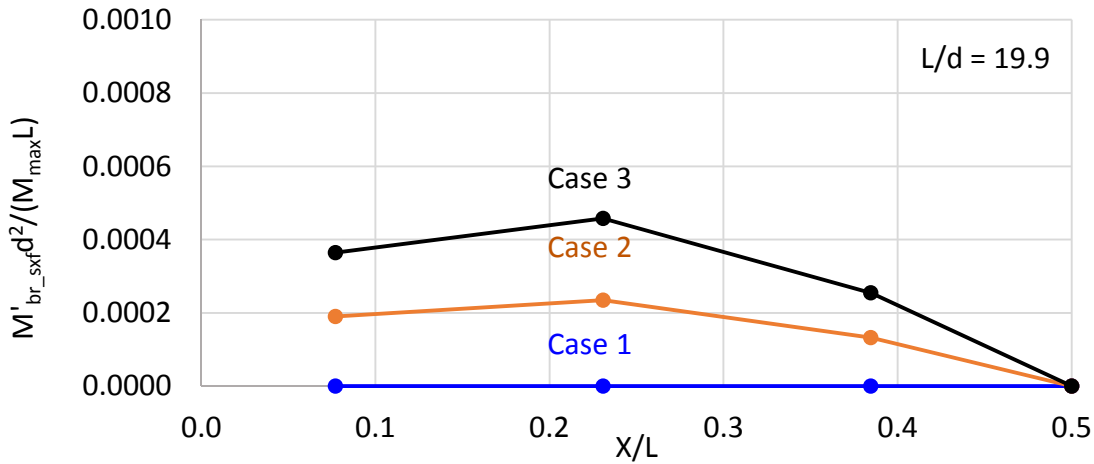


Figure 13: Normalized SXF Brace Moments along Girder Length

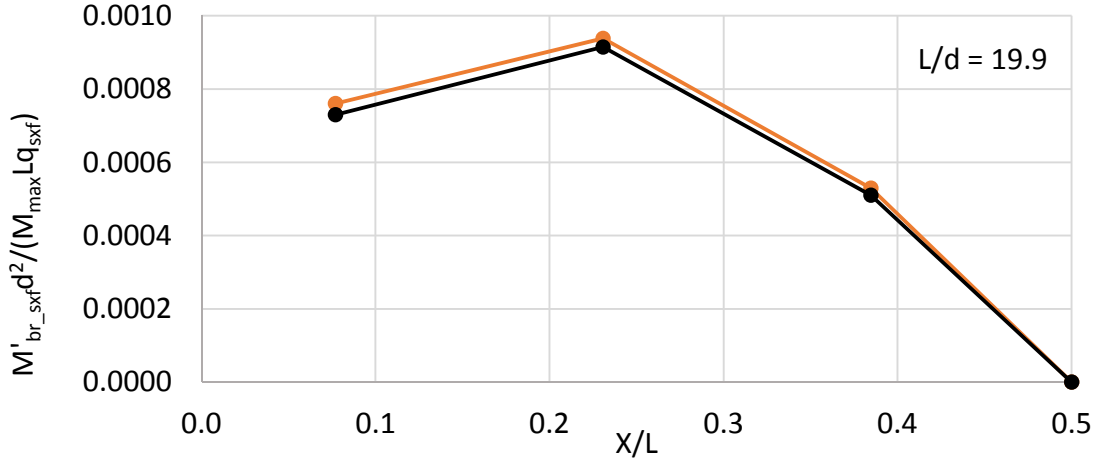


Figure 14: Further Normalized SXF Brace Moments along Girder Length

8. Connection Design Provisions for Stiffened PMDF Diaphragms

The next step in this ongoing research is to use the knowledge gained from the parametric study on brace moment distribution in a stiffened PMDF diaphragm to determine design provisions for the connections from the PMDF sheets to the stiffening angles and for the connections from the girders to the stiffening angles.

9. Conclusions

This paper summarized the results of a parametric study to determine the strength requirements of stiffened permanent metal deck form diaphragms utilized for stability bracing of girders. The strength requirements were based on a diaphragm stiffness of four times the ideal value and an initial girder twist imperfect of $\theta_0 = L/(500d)$. For simplicity, the stiffened diaphragms were modeled using cross-frames for the metal deck forms and rigid beams with stiffening cross-frames for the stiffening angles. The relative shear rigidity of the cross-frames versus the stiffening cross-frames was calibrated from the experimental test results of a previous study. From the parametric study which consisted of 24 models, both an expression for the maximum bracing moments of the cross-frames and an expression for the maximum bracing moments stiffening cross-frames were developed. Ongoing research is being conducted to determine a model for the fastener forces so that design provisions can be developed for the connections from the metal deck forms to the stiffening angles and for the connections from the stiffening angles to the girder.

References

- AISC. (2010). *Code of standard practice for steel buildings and bridges*, 14th Ed., Chicago.
- Currah, R. M. (1993). "Shear strength and shear stiffness of permanent steel bridge deck forms." M.S. Thesis, University of Texas, Austin.
- Egilmez, O. O. (2005). "Lateral bracing of steel bridge girders by permanent metal deck forms." PhD. Dissertation, Univ. of Houston, Houston.
- Egilmez, O., Helwig, T. A., and Herman, R. S. (2005). "Strength of metal deck forms used for stability bracing of steel bridge girders." *Proc., Structural Stability Research Council/North American Steel Construction Conf.*, Montreal, 257–276.
- Egilmez, O. O., Herman, R. S., and Helwig, T. A. (2009). "Lateral stiffness of steel bridge I-girders braced by metal deck forms." *Journal of Bridge Engineering*, 14(1) 17–25.
- Errera, S., and Apparao, T. (1976). "Design of I-shaped beams with diaphragm bracing." *Journal of the Structural Division*, 102(4), 769–781.
- Galambos, T. V., ed. (1998). *Guide to stability design criteria for metal structures*, 5th Ed., Wiley, New York.
- Helwig, T. A., and Frank., K. H., (1999). "Stiffness requirements for diaphragm bracing of beams." *Journal of Structural Engineering*, 125(11) 1249–1256.
- Helwig, T. A., Frank., K. H., and Yura, J. A. (1997). "Lateral-torsional buckling of singly-symmetric I-beams." *Journal of Structural Engineering*, 123(9) 1172–1179.
- Helwig, T. A., and Yura, J. A. (2008a). "Shear diaphragm bracing of beams. I: Stiffness and strength." *Journal of Structural Engineering*, 134(3) 348–356.
- Helwig, T. A., and Yura, J. A. (2008b). "Shear diaphragm bracing of beams. II: Design requirements." *Journal of Structural Engineering*, 134(3) 357–363.
- Nethercot, D., and Trahair, N. (1975). "Design of diaphragm-braced I-beams." *Journal of the Structural Division*, 101(10) 2045–2061.
- Yura, J. A. (2001). "Fundamentals of beam bracing" *Engineering Journal*, 38(1) 11-26
- Wang, L., and Helwig, T. A. (2005). "Critical imperfections for beam bracing systems." *Journal of Structural Engineering*, 131(6) 933–940.
- Winter, G. (1960). "Lateral bracing of columns and beams." *Transactions of the American Society of Civil Engineering*, 125, 809–825.